

Analytical Solution of Impulse Response Function on Moving Point to Predict Encounter Water Waves in Head Wave Condition

Md Shahidullah Kaiser, Takahito Iida

Dept. of Naval Architecture & Ocean Engineering, Osaka University, Osaka, Japan

E-mail: shahidullah_kaiser@naoe.eng.osaka-u.ac.jp

1 INTRODUCTION

Moving ships require accurate head wave prediction to avoid direct impact and capsizing by encounter water waves (Susaki *et al.*, 2017). Short-term prediction can reliably predict encounter water waves at a particular location over approximately 30s to 1min (Halliday *et al.*, 2005). Recently, an analytical solution of the impulse response function for finite-depth water waves at static points has been derived where the non-causal effect diminishes exponentially with distance (Iida and Minoura, 2022). According to this, a numerical prediction method on moving points has been explored by inverse discrete Fourier transform (Kaiser and Iida, 2022). In this paper, we propose an analytical solution to predict encounter waves on moving points by the impulse response function based on the finite-depth dispersion relation of water waves. We have performed both numerical and experimental comparisons to validate the proposed method.

2 ANALYTICAL SOLUTION

A two-dimensional deterministic wave prediction problem with horizontal and vertical planes, as illustrated in Fig.1, is considered. The constant depth d and the gravitational acceleration g are used to normalize the variables; non-dimensionalizations are utilized regarding d for spatial variables, $\sqrt{d/g}$ for time variables, and $\alpha = V/\sqrt{gd}$ is the Froude number. Waves propagate to the positive x -direction. The origin O is moving backward with a constant speed V . Since both points A and B are moving at the same forward speed V , the distance x between them remains constant. The free surface elevation $\xi_B(t)$ at point B is predicted using a convolution integral of the wave elevation $\xi_A(t)$ at point A and the impulse response function $h(t)$, as

$$\xi_B(t) = \int_{-\infty}^{\infty} h(\tau)\xi_A(t - \tau)d\tau \quad (1)$$

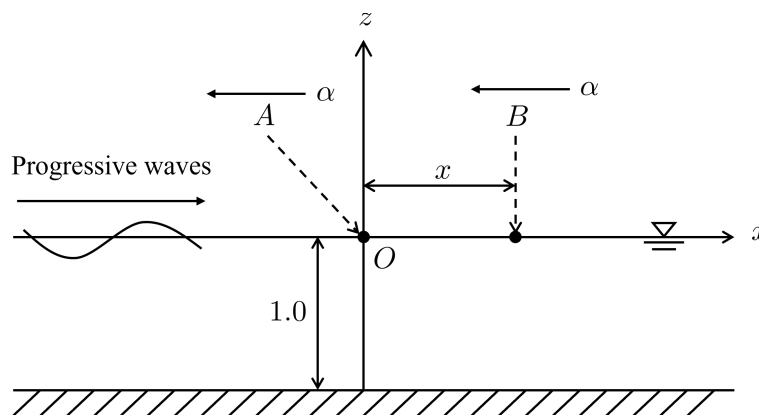


Fig. 1 Schematic view of two-dimensional water wave prediction problem. The distance between A and B is x , and the free surface displacement at point B is predicted from the time history of the displacement at point A .

The integral range for the causal impulse response function $h(t)$ is $[0, \infty]$, indicating that the present and past inputs determine the current outputs. The model is based on a linear time-invariant (LTI) system by assuming linear potential theory with small amplitude. The impulse response function is defined as $h(t) = (1/2\pi) \int_{-\infty}^{\infty} e^{i(\omega_e t - kx)} d\omega_e$ where ω_e is an encounter frequency and k is a wave number. Considering the head wave condition into account, the normalized relation between encounter frequency and incident wave frequency is represented as $\omega_e = \omega + \alpha\omega|\omega|$. The incident wave frequency ω is associated with the finite-depth dispersion relation $\omega|\omega| = k \tanh k$, and the phase function is $\phi = (\omega + \alpha\omega|\omega|)t - kx$. Due to the characteristics of the phase function, it is difficult to formulate a single analytical solution of the impulse response function for the whole time domain. Therefore, we propose a solution with three forms with respect to time which leads to the final outcome as

$$h(t) = \begin{cases} h_S(t) = C_1 \left[\cos \gamma \left\{ \text{Ai}[\beta] - \frac{\sin(\beta\chi)}{\pi\beta} \right\} + \sin \gamma \left\{ \text{Gi}[\beta] + \frac{\cos(\beta\chi) - 1}{\pi\beta} \right\} \right] \\ \quad + C_2 \left[\cos \gamma \left\{ \text{Gi}'[\beta] - \frac{\chi \sin(\beta\chi)}{\pi\beta} + \frac{1}{\pi\beta^2} (1 - \cos(\beta\chi)) \right\} \right] \\ \quad + \sin \gamma \left\{ -\text{Ai}'[\beta] + \frac{\chi \cos(\beta\chi)}{\pi\beta} - \frac{\sin(\beta\chi)}{\pi\beta^2} \right\} \quad (t \leq t_1) \\ \\ h_M(t) = D_1 \left[\cos \mu \left\{ \text{Ai}[\delta] - \frac{\sin(\delta\nu)}{\pi\delta} \right\} + \sin \mu \left\{ \text{Gi}[\delta] + \frac{\cos(\delta\nu) - 1}{\pi\delta} \right\} \right] \\ \quad + D_2 \left[\cos \mu \left\{ \text{Gi}'[\delta] - \frac{\nu \sin(\delta\nu)}{\pi\delta} + \frac{1}{\pi\delta^2} (1 - \cos(\delta\nu)) \right\} \right] \\ \quad + \sin \mu \left\{ -\text{Ai}'[\delta] + \frac{\nu \cos(\delta\nu)}{\pi\delta} - \frac{\sin(\delta\nu)}{\pi\delta^2} \right\} \quad (t_1 < t \leq t_2) \\ \\ h_L(t) = \text{Re} \left[\frac{1}{\pi} c_{gs} (1 + 2\alpha\omega_s) e^{i[(\omega_s + \alpha\omega_s^2)t - k_s x - \frac{\pi}{4}]} \sqrt{\frac{2\pi}{|t\omega_s'' + 2\alpha t\omega_s'^2 + 2\alpha t\omega_s\omega_s''|}} \right] \quad (t_2 < t \leq t_{\text{cut}}) \end{cases} \quad (2)$$

where

$$C_1 = \left(1 + \frac{4\alpha^2 t}{x}\right) \left(\frac{2}{x}\right)^{\frac{1}{3}}, \quad C_2 = 2\alpha \left(\frac{2}{x}\right)^{\frac{2}{3}}, \quad D_1 = \left(1 + 4\alpha^2\right) \left(\frac{2}{t}\right)^{\frac{1}{3}}, \quad D_2 = 2\alpha \left(\frac{2}{t}\right)^{\frac{2}{3}}$$

$$\beta = \left(x - t - \frac{2\alpha^2 t^2}{x}\right) \left(\frac{2}{x}\right)^{\frac{1}{3}}, \quad \gamma = \frac{8\alpha^3 t^3}{3x^2} - \frac{2\alpha t(x-t)}{x}, \quad \chi = -\alpha t \left(\frac{2}{x}\right)^{\frac{2}{3}}$$

$$\delta = \left\{x - (1 + 2\alpha^2)t\right\} \left(\frac{2}{t}\right)^{\frac{1}{3}}, \quad \mu = \frac{8\alpha^3 t}{3} - 2\alpha(x-t), \quad \nu = -\alpha t \left(\frac{2}{t}\right)^{\frac{2}{3}}$$

$$t_1 = x|_{h_S(t_1)=h_M(t_1)}, \quad t_2|_{h_M(t_2)=h_L(t_2)}, \quad t_{\text{cut}} = \frac{x}{\alpha} \left(1 - \frac{1}{\sqrt{1 + 4\alpha\omega_e}}\right) < \frac{x}{\alpha}$$

Here, $\text{Ai}[\cdot]$ and $\text{Gi}[\cdot]$ are the Airy function and the Scorer's function, while $\text{Ai}'[\cdot]$ and $\text{Gi}'[\cdot]$ represent their corresponding first derivative. The three forms of impulse response function $h_S(t)$, $h_M(t)$, and $h_L(t)$ are for the small, middle, and large time domains, respectively. They are plotted in Fig.2 (a) on their valid domains as well as on other domains. The Maclaurin series expansion, the shallow water assumption, and the stationary phase method are employed to obtain these three domain solutions. In the stationary phase method, c_{gs} is the group velocity, ω_s is the natural frequency, and k_s is the stationary wave number. From Fig.2 (a), it can be observed that the proposed theory is valid until when $h_L(t_1) > h_M(t_1)$. Otherwise, the middle solution will not exist. This is the limiting range of this proposed method. The comparison between the analytical solution (2) and the numerical solution obtained by IDFT for the whole time domain is shown in Fig.2 (b). It has been seen that the analytical and numerical solutions show good agreement with each other. However, a little discrepancy exists beyond t_{cut} , which is the cut-off frequency. Because after the t_{cut} , the analytical solution is regarded

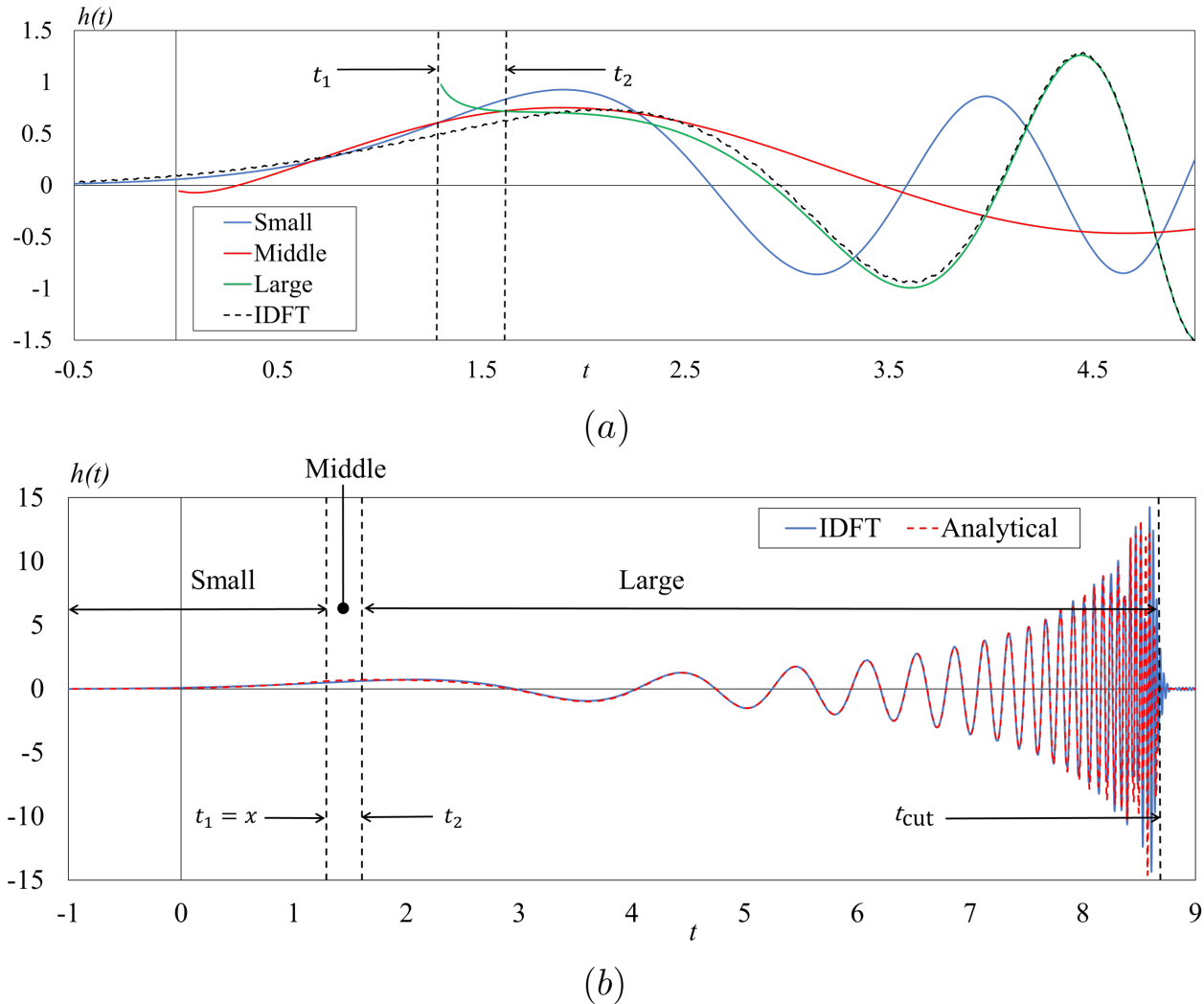


Fig. 2 Results are shown in the case of $x = 1.289$ and $\alpha = 0.134$. (a) Analytical solutions on small, middle, and large domains are plotted not only on their valid domains but also on other domains. (b) Comparison between the analytical solution of impulse response function and numerical solution by IDFT for the whole time domain.

as zero, while some residual value still exists in the numerical solution due to the involvement of the Gibbs phenomenon. Details of calculation processes and discussions about the limiting range are presented in the workshop.

3 PREDICTION OF IRREGULAR WAVES

A towing tank experiment was carried out to validate the proposed theories. The experiment was conducted in the towing tank at Osaka University, Japan. The length of the towing tank is 100 [m], and the width is 7.8 [m]. The tank is filled with pure water until the water level is 4.288 [m]. The distance between point A and B is 5.530 [m]. Therefore, the non-dimensional distance is $x = 5.530/4.288 = 1.289$. The sampling time was set as $\Delta t = 0.01$ [s]. The irregular wave's significant wave height was set to $H_{1/3} = 0.04$ [m], and the mean wave period was set to $T_{01} = 1.2$ [s]. The experiment was conducted at three different speeds 0.873, 1.061, and 1.238 [m/s]. After about 150 [s], the waves approached the carriage. Following that, the train began to move, and the carriage traversed approximately 70 [m] of distance. From Fig.3 (a), it can be observed that there is considerable agreement between predicted outputs by the analytical solution and experimental results.

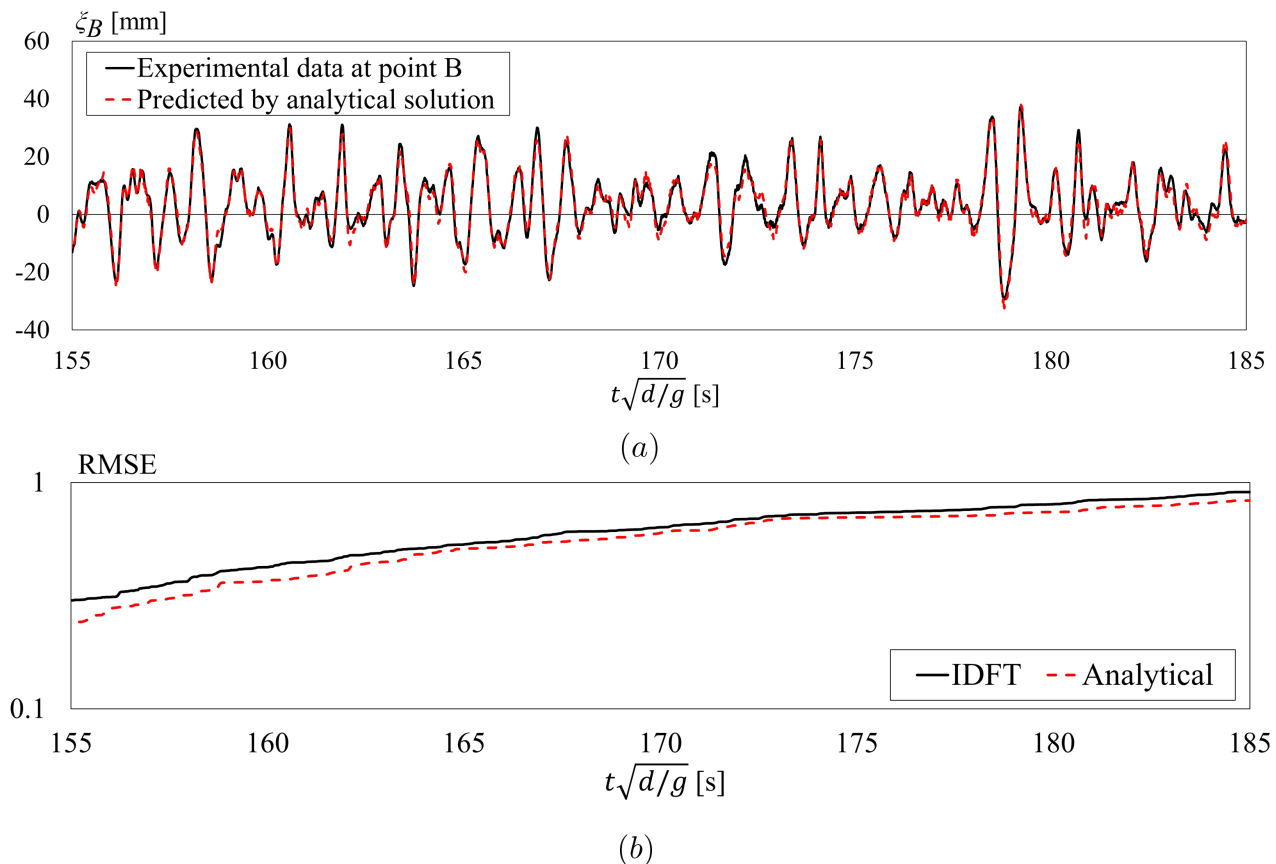


Fig. 3 (a) Prediction of irregular waves by the analytical solution of impulse response function at point B and comparison with experimental values, where $x = 1.289$ and $\alpha = 0.134$. (b) Root mean square error between experimental and predicted outputs (analytical and numerical impulse response functions of finite-depth water) on the semi-log graph.

In order to evaluate errors in the prediction models, a root mean square error (RMSE) is used as

$$\text{RMSE}(t) = \sqrt{\frac{1}{N_t(t)} \sum_{i=1}^N (\xi_{\text{pred.}} - \xi_{\text{exp.}})^2} \quad (3)$$

where $\xi_{\text{pred.}}$ and $\xi_{\text{exp.}}$ are the predicted elevation and that of experimental outputs respectively, and $N_t(t)$ is the number of time-series data at time t . The RMSE is shown on the semi-log graph in Fig.3 (b). Comparing the analytical and numerical solutions, the result of the analytical solution is smaller RMSE than that of the numerical outputs.

REFERENCES

- Halliday, J., Dorrell, D., & Wood, A., 2005. The Application of Short-Term Deterministic Wave Prediction to Offshore Electricity Generation, *Renewable Energy and Power Quality Journal*, 1, 10.24084.
- Iida, T., & Minoura, M., 2022. Analytical solution of impulse response function of finite-depth water waves, *Ocean Engineering*, 249, 110862.
- Kaiser, M. S., & Iida, T., 2022. Moving Point Prediction of Linear Irregular Water Waves Using Numerical Impulse Response Function. *The 32nd International Ocean and Polar Engineering Conference*, 5-10 June, Shanghai, China.
- Susaki, H., Hirakawa, Y., Takayama, T., & Hirayama, T., 2017. Acquisition and prediction of wave surface by marine radar for the safety of small ships, *Proceedings of the 16th International Ship Stability Workshop*, 5-7 June, Belgrade, Serbia.